



Vibroacoustics of a cavity coupled with an uncertain composite panel

C. Chen, Denis Duhamel, Christian Soize

► To cite this version:

C. Chen, Denis Duhamel, Christian Soize. Vibroacoustics of a cavity coupled with an uncertain composite panel. Soize, C; Schueller, GI. 6th International Conference on Structural Dynamics, Sep 2005, Paris, France. Millpress science Publishers, PO BOX 84118, 3009 CC Rotterdam, Netherlands, 1-3, pp.Pages: 859-864, 2005. <hal-00686195>

HAL Id: hal-00686195

<https://hal-upec-upem.archives-ouvertes.fr/hal-00686195>

Submitted on 8 Apr 2012

HAL is a multi-disciplinary open access archive for the deposit and dissemination of scientific research documents, whether they are published or not. The documents may come from teaching and research institutions in France or abroad, or from public or private research centers.

L'archive ouverte pluridisciplinaire **HAL**, est destinée au dépôt et à la diffusion de documents scientifiques de niveau recherche, publiés ou non, émanant des établissements d'enseignement et de recherche français ou étrangers, des laboratoires publics ou privés.

Vibroacoustics of a cavity coupled with an uncertain composite panel

C. Chen

Université de Marne-la-Vallée, Paris, France

D. Duhamel

Ecole Nationale des Ponts et Chaussées, Paris, France

C. Soize

Université de Marne-la-Vallée, Paris, France

ABSTRACT: This paper deals with uncertainties in vibroacoustics of a bounded cavity whose wall is constituted of a rigid wall and of a deformable part constituted of a Composite Sandwich Panel (CSP). Such a CSP has two thin carbon-resin skins and one high stiffness closed-cell foam core. The objectives of this paper is (1) to study the robustness of acoustic response with respect to the dispersion of the CSP induced by the manufacturing process, (2) to develop a predictive mean mechanical model of the vibroacoustic system and (3) to use a nonparametric probabilistic approach for data and model uncertainties of the CSP in order to analyze the robustness of the mean vibroacoustics model in the LF and MF bands to predict internal acoustic level.

1 INTRODUCTION

The numerical prediction of the response of vibroacoustic systems with composite sandwich panels is relatively robust with respect to data and model uncertainties in the low-frequency (LF) range, but is sensitive and then not robust to these uncertainties in the medium-frequency (MF) range. In this paper, we present some experimental results which allow (1) to analyze the robustness of the prediction of the internal acoustic level with respect to the dispersion of the composite panels induced by the manufacturing process, (2) to identify the dispersion parameters of nonparametric probabilistic model for uncertainties of the composite panel (Inverse problem), and (3) to compare the numerical prediction of the vibroacoustic system with experimental measurements. We are only interested in studying the influence of model uncertainties of the composite panel to the internal noise. The structure is a cube constituted of 5 rigid walls and one elastic wall corresponding to a composite panel. This structure is coupled with an internal acoustic cavity filled by gas (air). The excitation of this vibroacoustic system is a given dynamic force applied to the composite panel. The measured observations are the normal acceleration in several points of the composite panel and the acoustic pressure in several points in the internal acoustic cavity. The identification of the experimental fre-

quency response functions (FRF) is done by using the usual experimental method and the first eigenmodes and eigenfrequencies are identified using the experimental modal analysis (McConnell 1995, Ewins 1984, Balmes 2000). The mean mechanical model of the composite panel is developed by using the multi-layer thin plate theory (Ochoa and Reddy 1992, Reddy 1997, Jones 1999). The internal acoustic fluid is modelled by the Helmholtz equation in pressure with an additional dissipative term (Ohayon and Soize 1998, Lesueur 1988). Model and data uncertainties of the composite panel are taken into account by using the nonparametric probabilistic approach (Soize 2000, 2001), which has previously been used for studying this composite panel *in vacuo* (Chen *et al.* 2004a, b).

2 VIBROACOUSTIC SYSTEM AND EXPERIMENTS

The vibroacoustic system is constituted of a composite sandwich panel, a rigid wall and an internal acoustic cavity. The mean surface of the composite sandwich panel is the plane Oxy . The total thickness of the multilayer composite panel is 0.01068 m . Its length is 0.40 m , and its width is 0.30 m . This composite panel is coupled with the internal acoustic cavity which is a cube of 0.39 m length, 0.29 m width and 0.30 m depth. The five other walls of the cube are rigid. The composite panel (defined in (Chen *et al.* 2004a, b)) is

constituted of two thin carbon-resin skins and a cell-closed foam core relatively rigid. Each skin is constituted of two thin plies in carbon-resin, each ply is 0.00017 m thickness, has a mass density 1600 Kg/m^3 and whose elasticity constants are $E_x = 101\text{ GPa}$, $E_y = 6.2\text{ GPa}$, $\nu_{xy} = 0.32$, $G_{xy} = G_{xz} = G_{yz} = 2.4\text{ GPa}$. The first two layers are unidirectional carbon-resin plies and are oriented in $[60/-60]$. The third layer is the foam with 0.01 m thickness, a mass density of 80 Kg/m^3 and elasticity constants $E_x = E_y = 60\text{ MPa}$, $\nu_{xy} = 0$, $G_{xy} = G_{xz} = G_{yz} = 30\text{ MPa}$. The fourth and fifth layers are two unidirectional carbon-resin plies in a $[60/-60]$ layout. The experimental model of the vibroacoustic system is shown in Fig. 1. The panel is vertical in the plane Oxy . The origin O is located in the lower left corner of the panel. The y -axis is vertical. The acoustic cavity is on the left of the photo. It can be seen in the right of the photo the electro-dynamical shaker which delivers the excitation force following the z -axis which is perpendicular to the plan of the panel. This force is located at the point P_0 with co-ordinates $x = 0.187\text{ m}$, $y = 0.103\text{ m}$. In this paper, the results presented are limited to normal accelerations to the panel in two points among the 25 measured points and to acoustic pressures inside the acoustic cavity in two points among the 16 measured points. The two observation points in the composite panel are P_1 of co-ordinate $x = 0.187\text{ m}$, $y = 0.159\text{ m}$ and P_2 of co-ordinate $x = 0.337\text{ m}$, $y = 0.272\text{ m}$. The two observation points in the acoustic cavity are C_1 of co-ordinate $x = 0.310\text{ m}$, $y = 0.104\text{ m}$, $z = 0.119\text{ m}$ and C_2 of co-ordinate $x = 0.135\text{ m}$, $y = 0.104\text{ m}$, $z = 0.021\text{ m}$.



Figure 1. Photo of experimental model of the vibroacoustic system

3 REDUCED MEAN MODEL OF THE VIBROACOUSTIC SYSTEM

For all frequency ω fixed in the frequency band of analysis, the reduced mean model of the vibroacoustic

system can be written (Ohayon and Soize 1998) as

$$\begin{bmatrix} [\underline{A}^S(\omega)] & i\omega[\underline{C}] \\ i\omega[\underline{C}]^T & -[\underline{A}^F(\omega)] \end{bmatrix} \begin{bmatrix} \underline{\mathbf{q}}^S(\omega) \\ \underline{\tilde{\mathbf{q}}}^F(\omega) \end{bmatrix} = \begin{bmatrix} \underline{F}^S(\omega) \\ 0 \end{bmatrix} \quad (1)$$

in which $\underline{\mathbf{q}}^S(\omega)$ is the complex vector of the n generalized co-ordinates of the structure, $\underline{\tilde{\mathbf{q}}}^F(\omega)$ is the complex vector of the m generalized co-ordinates of acoustic cavity. The generalized dynamical stiffness matrix $[\underline{A}^R(\omega)]$ with $R = S$ or $R = F$ can be written as

$$[\underline{A}^R(\omega)] = -\omega^2[\underline{M}^R] + i\omega[\underline{D}^R] + [\underline{K}^R] \quad , \quad (2)$$

in which $[\underline{M}^R]$, $[\underline{D}^R]$, $[\underline{K}^R]$ are generalized mass, damping and stiffness matrices. The matrix $[\underline{C}]$ is a $(n \times m)$ real matrix corresponding to the generalized vibroacoustic coupling. The displacement vector of the composite panel and the acoustic pressure vector in the acoustic cavity are such that

$$\underline{U}^S(\omega) = [\underline{\Psi}]\underline{\mathbf{q}}^S(\omega) \quad , \quad \underline{P}^F(\omega) = i\omega[\underline{\Phi}]\underline{\tilde{\mathbf{q}}}^F(\omega) \quad , \quad (3)$$

in which $[\underline{\Psi}]$ is the $(n_S \times n)$ real matrix constituted of the 6 rigid body modes of the composite panel and of the $(n - 6)$ elastic modes of the composite panel *in vacuo* associated with the $(n - 6)$ first eigenfrequencies. The $(n_F \times m)$ real matrix $[\underline{\Phi}]$ is constituted of the constant pressure mode associated with zero eigenvalue and of the acoustic modes associated with the $(m - 1)$ first acoustic eigenfrequencies of the internal acoustic cavity with rigid walls. In addition, n_S and n_F are the number of degrees of freedom for the composite panel and for the internal acoustic cavity, corresponding to a finite element mesh of the vibroacoustic system. The mesh of the 2D composite panel is constituted of 64×48 four-nodes finite elements for laminated plate bending. The mesh of the 3D internal acoustic cavity is constituted of $62 \times 46 \times 30$ eight-nodes acoustic finite elements. The meshes are compatible on the vibroacoustic interface.

4 NON PARAMETRIC PROBABILISTIC APPROACH FOR DATA AND MODEL UNCERTAINTIES OF THE COMPOSITE PANEL

Using the nonparametric probabilistic approach for data and model uncertainties introduced in reference (Soize 2000, 2001), for the composite panel, Eq. (1) is replaced by the following random equation,

$$\begin{bmatrix} [\underline{\mathbf{A}}^S(\omega)] & i\omega[\underline{\mathbf{C}}] \\ i\omega[\underline{\mathbf{C}}]^T & -[\underline{\mathbf{A}}^F(\omega)] \end{bmatrix} \begin{bmatrix} \underline{\mathbf{Q}}^S(\omega) \\ \underline{\tilde{\mathbf{Q}}}^F(\omega) \end{bmatrix} = \begin{bmatrix} \underline{F}^S(\omega) \\ 0 \end{bmatrix} \quad (4)$$

in which, $\underline{\mathbf{Q}}^S(\omega)$ and $\underline{\tilde{\mathbf{Q}}}^F(\omega)$ are the complex random vectors of the generalized co-ordinates. In Eq (2), the

mean generalized dynamical stiffness matrix $[A^S(\omega)]$ of the composite panel with uncertainties has been replaced by the following complex random matrix

$$[A^S(\omega)] = -\omega^2[M^S] + i\omega[D^S] + [K^S] \quad (5)$$

in Eq. (5), the probability distributions of the full random matrices $[M^S]$, $[D^S]$, $[K^S]$ are explicitly defined. The dispersion of random matrices $[M^S]$, $[D^S]$, $[K^S]$ is controlled by the positive-valued dispersion parameters δ_M , δ_D and δ_K . The random acoustic pressure vector in the cavity and the random displacement vector of the composite panel are written as

$$U^S(\omega) = [\Psi] Q^S(\omega), \quad P^F(\omega) = i\omega [\Phi] \tilde{Q}^F(\omega). \quad (6)$$

Equations (4) to (6) define the stochastic reduced model associated with the reduced mean model defined by Eqs. (1) to (3).

5 EXPERIMENTAL ESTIMATION OF DISPERSION PARAMETERS OF THE NONPARAMETRIC PROBABILISTIC APPROACH FOR DATA AND MODEL UNCERTAINTIES IN THE COMPOSITE PANEL

The method used to identify the dispersion parameters δ_M , δ_D and δ_K which is developed and applied to the composite panel *in vacuo* in the references (Chen *et al.* 2004a, b), is briefly summarized below. For the composite panel, the method consists in associating with the ν first elastic modes computed with the mean finite element model, the corresponding ν experimental elastic modes obtained from the experimental modal analysis. Since the experimental elastic modes differ from the elastic modes computed with the mean finite element model, the following transformation of basis is introduced:

$$\tilde{\mathbf{q}}^{exp}(\theta_r) = [S_\nu^{exp}(\theta_r)] \mathbf{q}^{exp}(\theta_r) \quad (7)$$

in which, $\tilde{\mathbf{q}}^{exp}(\theta_r)$ is the \mathbb{C}^m -vector of the experimental generalized coordinates for composite panel θ_r , and where $\mathbf{q}^{exp}(\theta_r)$ is the corresponding \mathbb{C}^m -vector of the generalized coordinates in the mean-model basis. The transformation defined by Eq. (7) allows the experimental generalized mass, damping and stiffness matrices $[\tilde{M}_\nu^{exp}(\theta_r)]$, $[\tilde{D}_\nu^{exp}(\theta_r)]$ and $[\tilde{K}_\nu^{exp}(\theta_r)]$ to be transformed into the matrices $[M_\nu^{exp}(\theta_r)]$, $[D_\nu^{exp}(\theta_r)]$ and $[K_\nu^{exp}(\theta_r)]$ which are expressed in the same vector subspace than $[M_\nu^S]$, $[D_\nu^S]$ and $[K_\nu^S]$. The random matrices $[M_\nu^S]$, $[D_\nu^S]$ and $[K_\nu^S]$ correspond to random matrices $[M^S]$, $[D^S]$ and $[K^S]$ for $n = \nu$.

Let A be M , D or K . Let $[G_\nu^{exp}(\theta_r)]$ be the positive-definite $n \times n$ real matrix such that $[A_\nu^{exp}(\theta_r)] = [\underline{L}_{A_\nu}]^T [G_\nu^{exp}(\theta_r)] [\underline{L}_{A_\nu}]$ in which the invertible upper triangular $n \times n$ real matrix $[\underline{L}_{A_\nu}]$ is such that

$[\underline{A}_\nu] = [\underline{L}_{A_\nu}]^T [\underline{L}_{A_\nu}]$. Therefore, matrix $[G_\nu^{exp}(\theta_r)]$ can be written as

$$[G_\nu^{exp}(\theta_r)] = [\underline{L}_{A_\nu}]^{-T} [A_\nu^{exp}(\theta_r)] [\underline{L}_{A_\nu}]^{-1} \quad (8)$$

For a fixed value of ν , the dispersion parameter δ_A of random matrix $[A_\nu^S]$ can then be estimated by

$$\delta_A(\nu) = \left\{ \frac{1}{8\nu} \sum_{r=1}^8 \|[G_\nu^{exp}(\theta_r)] - [I_\nu]\|_F^2 \right\}^{1/2}, \quad (9)$$

in which $\|[B]\|_F^2 = tr\{[B]^T[B]\}$ is the square of the Frobenius norm of the matrix $[B]$ and where $[I_\nu]$ is the $\nu \times \nu$ identity matrix. The dispersion parameter δ_A of random matrix $[A^S]$ is then defined by

$$\delta_A = \min_{\nu \geq 2} \delta_A(\nu) \quad (10)$$

Fig. 2 displays the graphs of functions $\nu \mapsto \delta_M(\nu)$, $\nu \mapsto \delta_D(\nu)$ and $\nu \mapsto \delta_K(\nu)$. It can be seen that the minima are obtained for $\nu = 5$ and consequently, Eq. (10) yields $\delta_M = 0.23$, $\delta_D = 0.43$ and $\delta_K = 0.25$ for random matrices $[M^S]$, $[D^S]$ and $[K^S]$ (these values are independent of dimension n of the stochastic reduced model).

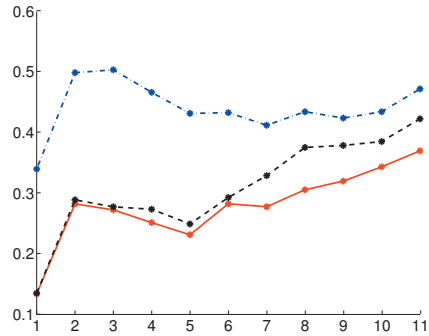


Figure 2. Graphs of functions $\nu \mapsto \delta_M(\nu)$ (solid line), $\nu \mapsto \delta_D(\nu)$ (dash-dot line) and $\nu \mapsto \delta_K(\nu)$ (dashed line). Horizontal axis: ν . Vertical axis: δ

6 CONFIDENCE REGION PREDICTIONS FOR THE VIBROACOUSTIC FREQUENCY RESPONSE FUNCTIONS AND EXPERIMENTAL COMPARISONS

6.1 Confidence region prediction with the nonparametric probabilistic model

We are interested in the construction of the confidence region associated with a probability level $P_c = 0.98$ (1) for the modulus of the random cross-frequency response functions (in acceleration) between driven point P_0 and observation points P_1 and P_2 , and (2)

for the modulus of the random cross-frequency response functions (in pressure) between driven point $P0$ and observation points $C1$ and $C2$. Let $W(\omega)$ representing one of the four quantities introduced above. The confidence region is constructed by using the quantiles. For ω fixed in B , let $F_{W(\omega)}$ be the cumulative distribution function (continuous from the right) of random variable $W(\omega)$ which is such that $F_{W(\omega)}(w) = P(W(\omega) \leq w)$. For $0 < p < 1$, the p th quantile (or fractile) of $F_{W(\omega)}$ is defined as

$W(\omega; \theta_1), \dots, w_{n_s}(\omega) = W(\omega; \theta_{n_s})$ be the n_s independent realizations of random variable $W(\omega)$. Let $\tilde{w}_1(\omega) < \dots < \tilde{w}_{n_s}(\omega)$ be the order statistics associated with $w_1(\omega), \dots, w_{n_s}(\omega)$. Therefore, we have the following estimation

$$w^+(\omega) \simeq \tilde{w}_{j^+}(\omega), \quad j^+ = \text{fix}(n_s P_c) \quad (13)$$

$$w^-(\omega) \simeq \tilde{w}_{j^-}(\omega), \quad j^- = \text{fix}(n_s(1 - P_c)) \quad (14)$$

in which $\text{fix}(z)$ is the integer part of the real number z . Random Eq. (4) is solved by using the Monte Carlo

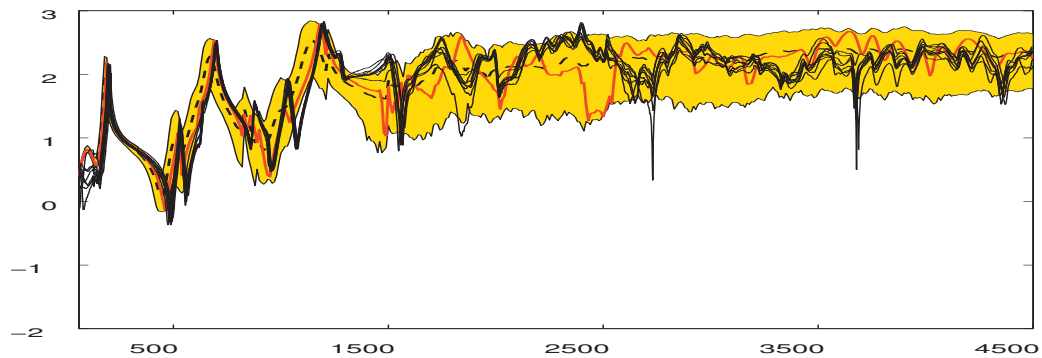


Figure 3. Confidence region for the normal acceleration at point P1 of the panel

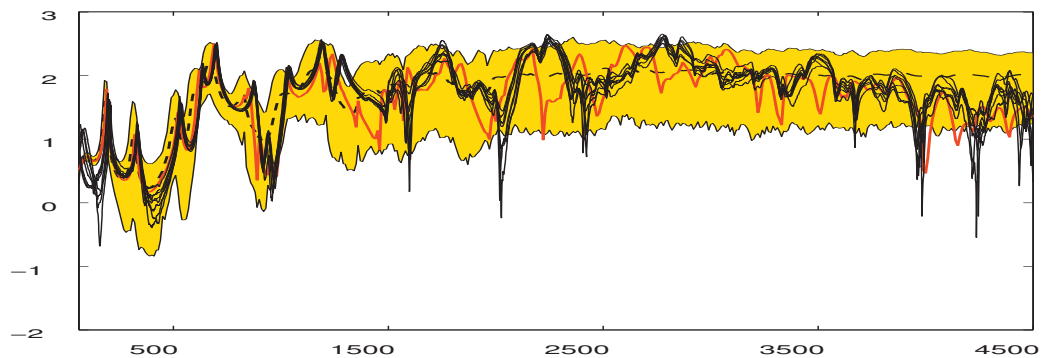


Figure 4. Confidence region for the normal acceleration at point P2 of the panel

$$\zeta(p) = \inf\{w : F_{W(\omega)}(w) \geq p\} \quad (11)$$

Then, the upper envelope $w^+(\omega)$ and the lower envelope $w^-(\omega)$ of the confidence region are defined by

$$w^+(\omega) = \zeta(P_c) \quad , \quad w^-(\omega) = \zeta(1 - P_c) \quad (12)$$

The estimation of $w^+(\omega)$ and $w^-(\omega)$ is performed by using the sample quantiles. Let $w_1(\omega) =$

numerical simulation with n_s realizations. The realization $\mathbf{Q}^S(\omega; a_\ell)$ of the \mathbb{C}^n -valued random variable $\mathbf{Q}^S(\omega)$ and the realization $\tilde{\mathbf{Q}}^F(\omega; a_\ell)$ of the \mathbb{C}^m -valued random variable $\tilde{\mathbf{Q}}^F(\omega)$ are the solution of the deterministic matrix equation

$$\begin{bmatrix} [\mathbf{A}^S(\omega; a_\ell)] & i\omega[\mathbf{C}] \\ i\omega[\mathbf{C}]^T & -[\mathbf{A}^F(\omega)] \end{bmatrix} \begin{bmatrix} \mathbf{Q}^S(\omega; a_\ell) \\ \tilde{\mathbf{Q}}^F(\omega; a_\ell) \end{bmatrix} = \begin{bmatrix} [\mathbf{F}^S(\omega)] \\ 0 \end{bmatrix} \quad (15)$$

with

$$[\mathbf{A}^S(\omega; a_\ell)] = -\omega^2[\mathbf{M}^S(a_\ell)] + i\omega[\mathbf{D}^S(a_\ell)] + [\mathbf{K}^S(a_\ell)]$$

in which $[\mathbf{M}^S(a_\ell)]$, $[\mathbf{D}^S(a_\ell)]$ and $[\mathbf{K}^S(a_\ell)]$ are the realizations of random matrices $[\mathbf{M}^S]$, $[\mathbf{D}^S]$ and $[\mathbf{K}^S]$ respectively. The confidence region of the random cross-frequency response functions are calculated by using Eqs. (13)-(15).

with respect to the number ν of realizations used in the Monte Carlo numerical simulation. These values are $n = 117$, $m = 630$ and $\nu = 1000$.

Figs. 3 and 4 display the modulus of the normal acceleration in \log_{10} at points P1(Fig.3) and P2(Fig.4) of the composite panel with respect to the frequency in Hertz. In each figure, the measurements of the eight panels are presented by the eight thin solid lines. The

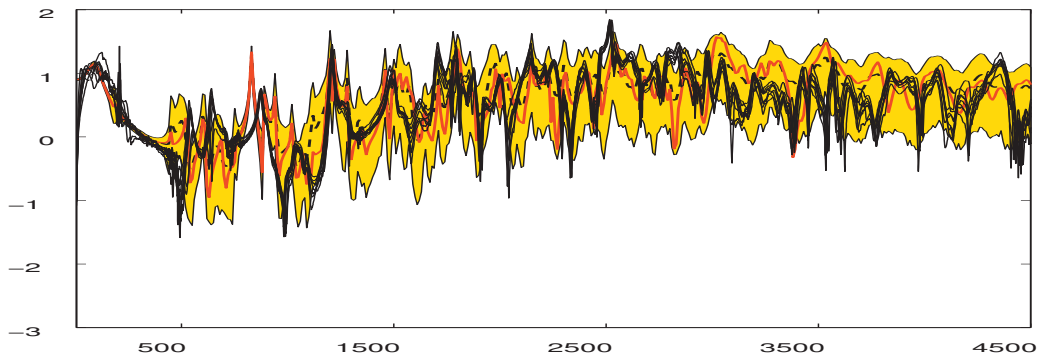


Figure 5. Confidence region for the acoustic pressure at point C1 inside the internal acoustic cavity

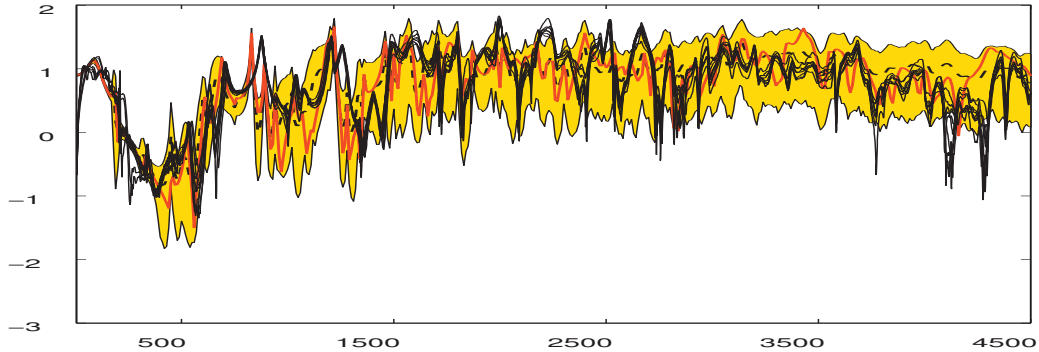


Figure 6. Confidence region for the acoustic pressure at point C2 inside the internal acoustic cavity

6.2 Comparison of numerical simulation with experimental results

The numerical results which are presented below correspond to the deterministic response of the reduced mean model and to the random response of the stochastic reduced model. The stochastic solution presented is converged with respect to dimensions n and m of the stochastic reduced model and

response of the mean model is the thick solid line. The mean value of the random response of the mean model is the dashed line. The confidence region for the probability level $P_c = 0.98$ is the grey region.

Figs. 5 and 6 display the modulus of the pressure in \log_{10} at points C1(Fig.5) and C2(Fig.6) inside the acoustic cavity with respect to the frequency in Hertz. In each figure, the measurements corresponding to the

eight panels are presented by the eight thin solid lines. The response of the mean model is the thick solid line. The mean value of the random response of the mean model is the dashed line. The confidence region for the probability level $P_c = 0.98$ is the grey region.

7 ANALYSIS AND CONCLUSION

The experimental analysis of the eight vibroacoustic systems, each one being constituted of a composite panel manufactured with the same process and of a same internal acoustic cavity, shows that the physical responses of the panel is relatively robust with respect to the manufacturing process in the frequency band $[0, 1000]$ Hertz. The robustness decreases with increasing frequency and the lack of robustness is significant in the frequency band $[3500, 4500]$ Hertz. This conclusion concerning robustness with respect to the manufacturing process of the composite panel for the dynamical response of the panel, holds for the acoustic response inside the acoustic cavity. It should be noted that the dispersion of the experimental responses of the composite panel propagates in the experimental acoustic response.

Concerning the robustness of the numerical prediction of the vibroacoustic response with respect to data and model uncertainties of the composite panel, the mean model is relatively robust in the frequency band $[0, 1000]$ Hertz and the robustness decreases with increasing frequency. The robustness is relatively poor in the frequency band $[1500, 4500]$ Hertz for the prediction of the composite panel responses. It can be seen that prediction of acoustic responses is likely more robust than the prediction of composite panel responses. This means that the structure uncertainties do not completely propagate in the internal acoustic cavity.

Finally, the comparisons of the experimental responses with the responses computed with the mean model show that the mean model gives a relatively good prediction in the frequency band $[0, 1000]$ Hertz. The quality of the mean model prediction is decreasing with increasing frequency and can be considered as bad in the frequency band $[2000, 4500]$ Hertz. The comparisons of the experimental responses with the stochastic responses computed with the stochastic model is relatively good. The nonparametric probabilistic approach which is proposed for taking into account data and model uncertainties in the composite panel allows the robustness of the numerical prediction to be improved.

REFERENCES

- Balmes, E. 2000. *Structural Dynamics Toolbox for Use with Matlab*. Scientific Software.
- Ewins, D. 1984. *Modal Testing: Theory and Practice*. John Wiley and Sons, Inc.
- Jones, R.M. 1999. *Mechanics of Composite Material*. Taylor and Francis.
- Lesueur, C. 1988. *Rayonnement Acoustique des Structures*. Eyrolles.
- McConnell, K. 1995. *Vibration Testing. Theory and Practice*. Wiley Interscience.
- Ochoa, O.O. & Reddy, J.N. 1992. *Finite Element Analysis of Composite Laminates*. Kluwer Academic Publishers.
- Ohayon, R. & Soize, C. 1998. *Structural Acoustics and Vibration*. Academic Press.
- Reddy, J.N. 1997. *Mechanics of Laminated Composite Plates*. CRC Press.